Journal of Infectious Diseases & Therapy Open access

Research Article

Experimental Multidrug Treatment of Chagas Disease

Antonio R. L. Teixeira*

Chagas Disease Multidisciplinary Research Laboratory, Center for Advanced Studies, University of Brasilia, Federal District, Brazil

***Correspondence**: Antonio R. L. Teixeira, Chagas Disease Multidisciplinary Research Laboratory, Center for Advanced Studies, University of Brasilia, Federal District, Brazil

Abstract

The protist *Trypanosoma cruzi* inserts kinetoplast DNA (kDNA) minicircle sequences into the host genome and the mutations generate genetically driven Chagas disease in chicken's refractory to the parasite infection. Chicks hatched from *T. cruzi* inoculated eggs retained the kDNA in the embryonic germ line cells and developed parasite- free Chagas disease-like cardiomyosspathy. Sensitive PCR with specific primer sets revealed protozoan kDNA in agarose gel bands probed with radiolabel-specific sequences for tissues of *T. cruzi* infected rabbits and mice. A target-primer TAIL-PCR with specific primer sets, southern hybridization, cloning and sequencing of the amplification products revealed kinetoplast minicircle sequences integration sites mainly in LINE-1 transposable elements and hitchhiking to several loci. This kinetoplast DNA biomarker was used to monitor the effect of multidrug treatment of *T. cruzi* infected mice. Nine out of 12 inhibitors prevented the kinetoplast DNA integration into the macrophage genome. A trypanocidal nitro heterocyclic compound and an array of eukaryotic cell divisions prevented minicircle sequence transfer. A trypanocidal nitro heterocyclic compound, combined with various eukaryotic cell division inhibitors, prevented minicircle sequence transfer. The multidrug treatment of *T. cruzi* infected mice with benznidazole, azidothymidine and ofloxacin lowered the rate of minicircle sequence integrations into the mouse genome by 2.44-fold. It reduced the rejection of the target heart cell.

Keywords: *Trypanosoma cruzi*; kDNA transfer; Biomarker; Multidrug treatment; Chagas disease

Received date: Feb 05, 2025; **Accepted date:** Feb 16, 2025; **Published date:** Feb 30, 2025

Citation: Teixeira ARL (2025) Experimental Multidrug Treatment of Chagas Disease. J Infect Dis Ther. 4:2.

INTRODUCTION

Chagas disease and American trypanosomiasis infections span an extensive geographical area in the American continent. Autochthonous, zoonotic *T. cruzi* infection spreads among mammal species. Human migration spreads the Chagas disease to five continents. The *Trypanosoma cruzi* agent of Chagas disease is a protist flagellate showing a symbiotic mitochondrion with circa a dozen maxicircles and twenty thousand catenated minicircles. The thousand copies of minicircles average 1.4 kb in size, each with four conserved 238 base pairs (bp) regions interspersed by four variable sequences of 122 bp intercalated sequence blocks CSB1, CSB2 and CSB3.

Individuals with flagellates in their blood usually do not perceive early-phase *T. cruzi* infections in humans. Life-long infections can occur in the absence of overt symptoms and signs. However, approximately one-third of chronically *T. cruzi*-infected humans develop clinical disease. The disease affects the heart (94.5% and the digestive system (megaesophagus and megacolon syndromes, 5.5%. The family-based Chagas disease is a prevalent cause of heart failure in the western hemisphere. The lead heterocyclic benzyl imidazole [N- Benzyl-2-(2-nitro-1H-imidazol-1-yl acetamide] has been used for the treatment of *T. cruzi* infections. The nitro heterocyclic killing of eukaryotic cells stems from reductase enzyme nitro anion radicals (R- (NO^{2-} and free O^{2-}, OH^{-} and H^2O^{2-}. The rodent (*Mus musculus* model is mainly used to monitor the treatment of the disease. Rabbits (*Oryctolagus cuniculus* are relatively resistant to early infection but die of chronic Chagas heart disease [1-3].

This study investigated the pathogenesis of the hallmark Chagas-like cardiomyopathy in a chicken model system refractory to T. cruzi infections. The chicks that hatched from T. cruzi-infected eggs integrated the kDNA minicircle sequences in their genomes and died of chronic Chagas-like heart disease. Herein, we advance the hypothesis that kDNA integration in the hosts' genome is a pathology biomarker; therefore, Chagas heart disease requires multidrug treatment with a trypanocide drug mixed with inhibitors of eukaryotic cell growth and differentiation.

The hypothesis to prevent the Chagas disease pathological manifestations is set forward, which consists of multidrug treatment with a lead nitro heterocyclic to inhibit the parasitic load and the integration of kDNA minicircle sequence with inhibitors of metabolic pathways of eukaryotic cell growth. The investigations revealed *Trypanosoma cruzi* kDNA minicirclesequence integrations in transposable elements of the host's genome. Treating *T. cruzi* infected mice with benznidazole, azidothymidine and ofloxacin lowered the ratio of kDNA mutations. Consequently, the *T. cruzi*-infected and treated mice displayed no or minimal rejection of heart cells by immune lymphocytes.

MATERIALS AND METHODS

Growth of eukaryotic cells

The Berenice *T. cruzi* was grown in 5 ml of Liver-Infusion Tryptose (LIT) medium in screw-cap glass tubes kept on a shaker-incubator at 27° C and a clone of the Tulahuen *T. cruzi* stock expressing β-galactose was grown in complete Dulbecco Minimum Essential Medium (cDMEM).

The *T. cruzi* epimastigotes grown in axenic LIT medium were employed to determine the optimal drug inhibitors for cell growth and development. The 4 *Leishmania brasiliensis* LTB300 stock promastigote forms harvested in the exponential growth phase were collected from the culture medium; the cells were washed three times in PBS, pH 7.4, were collected by centrifugation and were used in the experiments. The L6 murine muscle cells and the human macrophage cell line U937 were maintained by serial passaging in sterile culture flasks containing freshly prepared cDMEM. The cell line grown in 15 mL culture flasks was inoculated with 10×10^4 trypomastigotes.

After several division cycles, the host cell-loaded amastigotes differentiated into trypomastigotes that emerged in the supernatant. The flagellates were collected by centrifugation at 3,000 × g for 15 min in a swing bucket rotor, were washed three times and resuspended in FBS-free DMEM. The trypomastigotes were used in *ex vivo* drug inhibitor experiments to infect the experimental animals and model Chagas disease. To investigate the macrophages *T. cruzi* interactions, aliquots of 10×10^4 uninfected macrophages grown in cDMEM, pH 7.2, were incubated at 37°C, forming monolayers in the culture flasks inoculated with 5×10^4 *T. cruzi* trypomastigotes in 5 mL of DMEM. On day 14 post-infection, the macrophages were released with 0.25 M trypsin, washed three times with PBS, pH 7.2 and subjected to DNA extraction [4].

Assessment of the cytotoxic effect of drug inhibitors on *T. cruzi* infected muscle cells

The L6 muscle cell monolayers grown in a glass chamber were inoculated with 10×10^3 trypomastigotes suspended in 3 mL DME. One week after *T. cruzi* inoculation, the muscle cells loaded with the dividing amastigotes were treated with a specific eukaryotic cell growth inhibitor concentration. The optimal drug concentration was determined in triplicate doseresponse assays, which showed absent, discrete, moderate or severe toxic effects on the *T. cruzi*-infected host cells during two weeks in a CO_2 incubator at 37° C. The concentration of the drug inhibitor that did not kill muscle cells was identified under an inverted microscope.

Hosts cells' DNA extraction

T. cruzi infected macrophage monolayers were collected by centrifugation and washed once with PBS, pH 7.4. After two washes with TBS (20 mM Tris-HCl pH 7.2, 0.5 M NaCl) the cell pellets were obtained by centrifugation at 1,500 × g for 15 min and resuspended in 2 mL extraction buffer (1 mM Tris-HCL, pH 8.0, 0.1 M EDTA, 0.5%SDS, 200 ng/mL RNase). Thereafter, proteinase K (100 µg/mL) was added and the incubation period was extended for 12 h. The cells in the pellet were subjected to two extractions with an equal volume of chlorophenol (Phenol:Chloroform:Isoamyl, 25:24:1) and a further extraction with chlorophyll (Chloroform:Isoamyl alcohol, 24:1) under light agitation at room temperature. The aqueous and organic phases were separated by centrifugation at 5,000 × g for 10 min. DNA was precipitated with a 1:10 volume of 3 M sodium acetate, pH 4.7 and a 2.5 volume of cold 100% ethanol. After 30 min of incubation at -80°C, the DNA was sedimented by centrifugation at 12,000 × g for 15 min. The DNA was washed twice with 70% cold ethanol and dried before resuspension in buffer (10 mM Tris-HCl, pH 8.0, 1 mM EDTA, pH 8.0). The DNA was subject to 1% gel electrophoresis and then stored at -4°C [5].

Trypanosoma cruzi and *Leishmania brasiliensis* nuclear DNA (nDNA)

The *T. cruzi* epimastigote and the *L. brasiliensis* promastigote were collected by centrifugation at 3,000 × g for 15 min. The pellets were washed twice in TBS (5×10^7 flagellates/mL) and resuspended in the extraction buffer. After one h at 37°C,

proteinase-K (100 µg/mL) was added and the incubation proceeded for 12 h, following the same steps as those of the host cells.

Trypanosoma cruzi mitochondrion DNA (kDNA)

kDNA was extracted from *T. cruzi* and *L. brasiliensis*. In brief, either 5×10^7 epimastigotes or equal quantities of promastigotes were washed three times in PBS, collected by centrifugation and resuspended in 630 µL of NET buffer (10 mM Tris HCL, 100 mM EDTA, 100 mM NaCl, pH 8.0). The cells underwent lysis with the addition of 70 µL of 10% SDS and 7 µL of 20 mg/mL proteinase-K. After incubation for an additional 12 h the lysate was homogenized by sheering and 690 µL of NET buffer with 100 µL 20% sucrose was added. The mix was centrifuged at 14,000 × g for 15 min and the supernatant was removed with a pipette tip. The remaining 30 µL was resuspended in NET buffer containing sucrose. The pellet was collected by centrifugation, resuspended in 100 µL of distilled water and subjected to subsequent extractions as described for the host cells. The kDNA was precipitated with 2.5 volumes of 100% ethanol and 0.1 volume of 3 M sodium acetate, pH 8.0. The pellet was washed twice with 70% ethanol and the kDNA resuspended in 200 µL of TE buffer and stored at 4°C.

Quantification, enzyme digestion and electrophoretic analysis of DNA

The DNA samples were quantified by the spectrophotometric method and the integrity and purity were demonstrated by 1% gel electrophoresis in TAE buffer (90 mM Tris-acetate, pH 8.0, 25 mM EDTA). The digestion of the DNA was carried out by restriction enzyme and 2 units of EcoR1 cut 1 µg of DNA. After 4 h of incubation, the DNA fragments separated by gel electrophoresis were excised from the gel and purified [6,7].

Southern blot

The purified DNA fragments were separated by electrophoresis in a 1% agarose gel and transferred by the alkaline capillarity method to the nylon membrane in a denaturing solution (0.4 M NaOH). After transferring, the DNA was dried out and fixed to the membrane at room temperature. The random primer labeling system radiolabeled the probes *via* the insertion of (α32P)-dATP in the DNA sequence synthesis with Klenow polymerase in the presence of hexamer random primers. The radiolabeled probes were purified by chromatography in a Sephadex G-10 column and the radioactivity confirmed by scintigraphy showed >108 counts/µg of the DNA. Membrane prehybridization was carried out for four h at 65°C in 0.5% SDS, 5X Denhardt solution with 100 µg salmon DNA.

PCR amplifications and hybridizations

The *T. cruzi* kDNA amplification with the specific primer sets S34/37 and S35/36 secured the kinetoplast minicircle sequence. The internal oligonucleotide constant region amplification was obtained from the *T. cruzi* kDNA, using primers S34 and S67 and the nested S35 antisense primer. The 330-bp kinetoplast minicircle constant region kCR probe was PCRamplified from the *T. cruzi* infected host cell DNA template with the primer S34/S67, cloned into the TA vector and sequenced. The primer set S34/37 amplified as little as 15 fg of the conserved and variable sequence of the kDNA minicircle from *T. cruzi* infected host cells. The *T. cruzi* telomere DNA (nDNA) 188 nt The *T. cruzi* nCR and kCR sequences with annealing nucleotides were employed for hybridization (Table 2). The PCR assays were conducted with a template DNA concentration 20-fold above the detection levels, with 10 ng of each pair of primers, 0.5 IU of Taq and 0.2 mM of each dNTP in a final volume of 25 µL. The kCR and the nCR probe radio label [α-^{32}P]-dATP showed a specific activity of three thousand ci/mM and maximum stringency 0.1% SSC and 0.1 SDS at 65°C for one hour.

The *T. cruzi* kDNA probe showed specific hybridization with the cloned kDNA minicircle in phage m13 mp8, but it did not hybridize with genes in plasmids pTC4, PTC1 and PK03. The amplicons were obtained with 200 ng of test DNA template and 10 ng of each primer set in the reaction buffer (50 mM KCl, 10 mM Tris HCL, pH 9.0, 1.5 mM $MgCl_2$, 0.2 mM dNTPs and 2.5 units of Taq-polymerase). *T. cruzi* and *L. brasiliensis* DNA were used as controls. The PCRs were conducted in agreement with previous work.

	Target	Sequence
kDNA		
S34	KDNA	ACA CCA ACC CCA ATC GAA CC
S67	KDNA	GGT TTT GGG AGG GG(G/C) (G/C)(T/G)TC
S35	KDNA	ATA ATG TAC GGG (T/G)GA GAT GC
S35 reverse	KDNA	GCA TCT CMC CCG TAC ATT AT
S67 reverse	KDNA	GAM SSC CCC TCC CAA AACC
S36	KDNA	GGT TCG ATT GGG GTT GGT G
nDNA		
Tcz1	Telomere	5' GAG CTC TTG CCC CAC ACG GGT GCT 3'
Tcz2	Telomere	5' CCT CCA AGC AGC GGA TAG TTC ACG 3'

Table 1: The *Trypanosoma cruzi* kinetoplast DNA and nuclear DNA primers.

Probe	Sequence
nCR	
Nucleus telomere	5' CGAGCTCTTGCCCACACGGGTGCTGCACTCGGCTGATCGTTTTCGAG CGCTGCT GCATCACACGTCCAAATTTTTGTTTCCCGATTGTGAATGG TGGGAGTCAGAGGCACTCTCTGTCAATATCTGTTTGCGTGTTCACACACTGGA CACCAAACAACCCTGAACTATCCGCTTGGA GGAATTCG3'
KCR	
Kinetoplast minicircle	5' TTTTGGTTTTGGTGGGAGGGGGCGTTCAAATTTTGGCCGAAAATTCATGCATC TCCCCCTACATTATTGGCCGAAAATGGGGGTTGTTCGAGGTGAGGTTCGATTG GGTGGTGTAAG 3'

Table 2: The *Trypanosoma cruzi* nucleus and kinetoplast DNA-derived probe sequences, with primer binding sites underlined.

The bands in the gels sequence probe was PCR amplified with Tcz1/Tcz2 primers and validated by southern blot with a radio-labeled nCR probe. The primer sets Tcz1/Tcz2 amplified as little as 10 fg of *T. cruzi* nDNA repetitive telomere sequences. The kDNA and nDNA specific primers and probes are shown in Tables 1 and 2.

were transferred to nylon membranes and hybridized with radio labeled specific probes. The sensitivity of the PCR with the primer sets Tcz1/Tcz2 was tested with serial dilutions of the *T. cruzi* nDNA highly repetitive telomere sequence [8-10].

Amplification of the integrated kDNA minicircle sequence

The method for amplifying kDNA minicircle sequence integration into genomic flanking regions used the kDNA primer sets in either a 5'-3' or 3'-5' combination. The fragments obtained by PCR amplifications from *T. cruzi*-infected rabbit tissues that hybridized with the radiolabeled specific kCR probe were characterized by sequencing. Second, a targeting primer thermal asymmetric interlaced- PCR (tpTAIL-PCR) method was used to amplify LINE-1 from the genomes of chickens and mice with specific primers combined with the successive kDNA minicircle internal primers. The LINE-1 primer concentration was 10-fold below that of the kDNA primers employed.

The primers anneal to a gamut of contigs to amplify the transposon families.

Rabbit model

Two-month-old male and female New Zealand white rabbits were fed pellet chow and water ad libitum and housed in

individual cages at 65% humidity and a temperature of 24°C in the animal room. The rabbits of groups A and B were inoculated subcutaneously with 2.5 × 10^6 *T. cruzi* trypomastigotes collected from the muscle cell cultures. The group C were uninfected controls. The *T. cruzi*-infected group A rabbits were untreated. The therapeutic effect of the nitro-heterocycle benznidazole was investigated in eight rabbits of group B. The *T. cruzi* infected rabbits in group B were treated with intraperitoneal injections of benznidazole (8 mg/kg body weight) for 60 days. The rabbits of groups A and B and uninfected control group C were subjected to clinical inspections for heart disease and necropsy. The tissues fixed in 5% formalin were embedded in paraffin, cut 5 µm thin sections, Hematoxylin-Eosin (H-E) staining and histopathological analysis [11].

Inoculation of naked kDNA in rabbits and fertile chicken eggs

Four 60 day-old-old rabbits were injected with 375 µg of kDNA minicircles or with 125 µg of a cloned kDNA sequence (GeneBank accession number AF399842). In addition, 30 fertile eggs received 15 ng of minicircles or 5 ng of cloned kDNA in the air chamber. The presence of kDNA in tissues was assayed by PCR.

Chicken model

In this investigation, white Ross fertile chicken eggs were infected with 100 *T. cruzi* trypomastigotes through a hole in the eggshell air chamber and sealed with adhesive tape. The mock control eggs received culture medium only. These eggs hatched after 21-day incubation in a chamber at 37°C, with 65% humidity, while rolling for 1 min every 30 min; this incubation occurred in a chicken room maintained at an average of 24°C, under positive pressure with filtered air and exhaust. The chicks hatched in the incubator, remained there for 24 h and thereafter, at 32°C for one month and grew to adulthood. In addition, F0 hens fertilized by artificial insemination laid eggs that hatched F1 chicks and the repeat insemination of adult F1 chicken eggs generated F2 chicks. The F0, F1 and F2 chickens were used in the experiments. We observed that the embryonic stem cell cultures from uninfected control chicken blast cells erupted from the zygote membrane six hours after the egg incubation. The embryo blast cells adhered to the plastic surface and grew at 37°C and 65% humidity upon infection with β-galactosidase-expressing *T. cruzi* trypomastigotes.

The DNA analysis was conducted with peripheral blood mononuclear cells and solid tissues from forty-eight chickens hatched from eggs inoculated with 100 *T. cruzi* forms and mock control chickens. These flocks grew to adulthood in cages and were fed commercial chow and water ad libitum.

DNA extraction and nucleic acids analyses: We extracted semen from roosters, from the embryo tissues of non-inseminated eggs at set points of incubation, from tissues of chickens hatched from *T. cruzi* inoculated eggs and from mock controls. Here, DNAs from the semen, heart, skeletal muscle and large bowel of *T. cruzi* inoculated eggs and from mock control chickens were employed. These genomic DNA samples were templates for PCR amplification performed in triplicate.

The nCR and kCR amplicons were resolved in 1.3% agarose gel, transferred to a nylon membrane and hybridized with a specific (µ32P)-dATP-radio labeled probe-a random primer labeling kit labeled the nCR and kCR probes.

Southern hybridization of DNA from the *T. cruzi*-infected, from mock control eggs and *T. cruzi* kDNA positive control was performed in agreement with protocols described elsewhere. The tpTAIL-PCR was conducted with kDNA primer sets s34/s67, s35/s35as and s67as/ s36, respectively, through three cycles of the reaction, each in combination with each chicken primer Gg1 to Gg6 and with XeCrs1 to XeCrs2 described in previous paper. The 11 product obtained during each cycle was validated by southern blot with the radio- labeled kCR probe and subjected to clone and sequence.

The primers anneal to a specific region of the chimera sequence (GB FN599618) in the locus NW_001471673.1 on chromosome 3. These primers at a 0.004 µM concentration and annealing temperature were combined with kDNA primers. Those clones showing hybridization with radio-labeled kDNA were sequenced. The tpTAIL- PCR was validated in a mix of *T. cruzi* kDNA with DNA from naïve control birds.

Chagas disease clinical and pathological findings: Clinical parameters in chickens hatched from *T. cruzi* infected eggs ($kDNA^+$) and in the healthy controls ($kDNA^-$) were detected by inspection and by arrhythmias and increasing heart size by Electrocardiography (ECG) recordings. A one-channel ECG apparatus with a standard one mV/cm and a 25 min/sec speed was used with electrodes under the wing pits and on the back of the legs. ECG recordings of frontal leads AVR, AVL and AVF and an assessment of mean electrical axis deviation to the left were obtained. These experiments were carried out with 35 kDNA+ and 22 kDNA- chickens. After death, each chicken was subjected to a necropsy and the heart weight was recorded. The tissues fixed in formalin and embedded in paraffin were cut into 5 µm sections and H-E stained for histopathology.

Mouse model

Groups of 8-two-month-old BALB/c, male and female, mice weighing 20 to 25 grams were separately housed in cages maintained at 24°C and 65% humidity, under pressure air exhaust and fed commercial pellets and water ad libitum. The mice in the experimental groups received intraperitoneal inoculations with 10×10^3 *T. cruzi* trypomastigotes harvested from L6 muscle cell cultures. The parasitemia in the *T. cruzi*-infected mice was determined by direct microscopic examination of the tail-blood under cover slip on a Neubauer cell counting. The 12 blood samples were collected on the 5th day post-infection and every 15 days until the 60th day. In addition, the demonstration of *T. cruzi* in the blood was secured by hemoculture in a screwcap glass culture tube containing 5 mL of blood-agar slant plus 5 mL of LIT medium overlay. These culture tubes were inoculated with 100 µL of blood drawn by heart puncture from *T. cruzi*-infected mice and kept in a shaker incubator at 27°C for 60 days. The cultures were examined by microscopy on the 20th, 40th and 60th days [12].

Tissue samples of *T. cruzi*-infected mice in the A, B and C groups had their body tissue subjected to DNA extraction and samples fixed in formalin were subjected to histopathology. These procedures searched for tissue lesions in *T. cruzi*-infected mice treated with drug inhibitors of eukaryotic cell growth and differentiation and in mock control mice.

Multi-drug treatment of the *T. cruzi*-infected mice: Groups of eight two-month-old BALB/c mice were used for the multidrug treatment of *T. cruzi* infection. Each mouse in groups A to H received intraperitoneal inoculation of 10^4 *T. cruzi* trypomastigotes derived from L6 muscle cell cultures. Mice in group A), were positive control, *T. cruzi*-infected, untreated. *T. cruzi*-infected mice in groups B to G received 0.86 mg benznidazole daily. In addition to benznidazole, each mouse group received an inhibitor of eukaryote cell growth: Azidothymidine, group C; ofloxacin, group D; and praziquantel, group E. Group A was the control group and no inhibitor was received. A

Inhibitor	Activity	Dose (µM)
Azido-thymidine	Intercalating thymidine in the DNA inhibits reverse transcription at G2M phase, caspase-3-reduced cell division inhibition and apoptosis	0.13
Bromodeoxiuridine	Intercalating Br-uridine at S phase stops cell cycle and cell growth	0.09
Colchicine	Suppression of tubulin assembly inhibits microtubule dependent cell division	0.12
Genisteine	ATP inhibition through Protein Tyrosine Kinase (PTK) and cell growth	0.037
Microcystin LR	Inhibits PP1 and PP2 serine/threonine phosphatase and cell growth	0.005
Mitomycin C	Inhibits PP1 adn PP2 serine/threonine/phosphatase	0.02
Polymerase inhibition		
Campthotecin	Downregulates S phase checkpoint by ATR/CHKI polimerase I (DNA gyrase)	0.14
Cycloheximide	Inhibits p38-activated protein kinase (MAKPK) and entry at G2M mitotic phase	17
Etoposide	Inhibits p38-activated protein kinase (MAKPK) and entry at G2M mitotic phase	0.08
Ofloxacin	4-fluoroquinolone affects polymerase II metabolic pathway at G@M phase and apoptosis	0.083
Praziquantel	Inhibits protein serine/threonine (PI3-K) and polymerase I and II	0.147
Staurosporine	Protein kinases (A, C, CAM and PI3K) inhibitor of growth at G1 phase	0.19

Table 3: Checkpoint inhibitors of cell growth and differentiation.

Detection of parasitemia: The parasitemia in *T. cruzi*-infected mice was determined by examination of the flagellates in a drop of tail-collected blood on the 5th day post-infection and thereafter every 15 days until the 60th day. The parasite counts in 5 uL of blood diluted sample 1:2 under a 2 × 2 coverslip on a hemocytometer determined by microscopy. Additionally, the

presence of latephase parasites was determined by hemoculture of 100 uL of blood collected through heart puncture at 20-, 40- and 60 days post-infection. The mortality of mice in the A-to-H groups was recorded and the deceased were subjected to necropsy and had their tissue samples subjected to DNA extraction and fixed in formalin to histopathology. The mice were sacrificed under anesthesia at the end of experiments at the 250th day of infection [13-15].

Detection of serum T. cruzi antibody: The T. cruzi antibody titters were revealed by the Enzyme-Linked Immunosorbent Assay (ELISA) as described elsewhere. A spectrophotometer was used for multidrug regimen was also administered to the following mice groups:

F) ofloxacin and azidothymidine. G) ofloxacin and praziquantel. H) azidothymidine and praziquantel. DNA from L. brasiliensis and uninfected mice were negative controls. DNA from T. cruzi was the positive control. The daily drug administration regimen was initiated on the fifth-day post-infection and continued for 60 days. Each drug powder stock was suspended in distilled water to the concentration indicated in Table 3 and the aliquot mix was administered through gavage with a 4 cm long urethral catheter n° 3.

G) plate reading at a wavelength of 480 nm. The optical density above a

H) 0.064 cut-off separated positive from adverse antibody reactions.

I) Extraction of DNA from Trypanosoma cruzi-infected, infected- treated and control uninfected mice: At the 250th-day-end experiment, the tissue samples from the heart, skeletal muscle, large intestine and spleen from each mouse were collected. Small fragments (approximately 200 mg) of each tissue were transferred to sterile dishes minced and transferred to sterile 15 mL screw-cap plastic tubes. DNA extraction from these samples was carried out stepwise according to the description in section 4.1. The PCR protocol for the nucleic acid-based diagnosis of T. cruzi infection with exact methods to identify the T. cruzi nuclear DNA (nDNA) in the tissues is described elsewhere.

J) Targeting primer thermal asymmetric interlaced PCR: The specific site of the kDNA minicircle sequence integration into the

human genome was identified by the tpTAIL-PCR. The study showed that 70.8% of the kDNA integrations occurred in retrotransposon LINE-1. Interestingly, the kDNA minicircle sequence integrated into the chicken CR-1 transposon. This information led to the unraveling

F)

Primer	Target	Family	Sequence (5'→3')
L1cam-5' UTR F Sense	5' UTR	F	ACC TTC CCT GTA AGA GGA GAG
L1cam-5' UTR F Antisense	5' UTR	F	GCT CTC CTC TTA CAG GGA AGG T
L1cam-5' UTR A Sense	5' UTR	A	GAC CTC TGG TGA GTG GAT CAC
L1cam-5' UTR A Antisense	5' UTR	A	GTG ATC CAC TCA CCA GAG GTC
L1cam-5' UTR T_F Sense	5' UTR	T_F	TTA GTC TGA ACA GGT GAG AGG
L1cam-5' UTR T_F Antisense	5' UTR	T_F	CCT CTC ACC TGT TCA GAC TAA
L1cam-5' UTR G_F Sense	5' UTR	G_F	GCG CCA TCT TCA GCT CCA GA
L1cam-5' UTR G_F Antisense	5' UTR	G_F	TCT GGA GCT GAA GAT GGC GC
L1 cam-2	ORF 1	All	CTA TGA AAG CCA GAA GAG CCT G
L1 cam-3	ORF 2	All	ACA GCC ACA AGA ACA GAA TGC
L1 cam-4	3' UTR	All	GCC TAG TCG GCC ATC ACT G
L1 cam-5 (L1 cam 4 Antisense)	3' UTR	All	CAG TGA TGG CCG ACT AGG C
L1 cam-6 (L1 cam 3 Antisense)	ORF 2	All	GCA TTC TGT TCT TGT GGC TGT
L1 cam-7 (L1 cam 2 Antisense)	ORF 1	All	CAG GCT CTT CTG GCT TTC ATA G
ORF2(01) Sense	ORF 2	All	GAG TGC CTC CAA GAA GAA ACG
ORF2(01) Antisense	ORF 2	All	CGT TTC TTC TTG GAG GCA CTC

ORF2(02) Sense	ORF 2	All	TCA TCC ATC CTG ACC AAG TAG G
ORF2(02) Antisense	ORF 2	All	CCT ACT TGG TCA GGA TGG TGA

Table 4: *Mus musculus* LINE-1 specific primers.

The mouse DNA samples were amplified after each reaction cycle initiated by the kDNA minicircle sequence primer combined with the mouse LINE retrotransposon-specific primer. The tpTAIL-PCR scheme covered the LINE 5' Short, Direct Repeat (SDR), the 3' and 5' Untranslated Regions (UTR), the Open Reading Frames (ORF1 and ORF2) and the poly-A tail (An) of LINE-1. In addition, the Conserved Sequence Block (CSB) conserved and variable regions, kDNA minicircle sequence amplification and mouse LINE DNA shown in previous paper.

Southern blot and radio labeled probe hybridization: The tpTAIL-PCR-amplified sequences were separated by electrophoresis in a 1% agarose gel and transferred to a positively charged nylon membrane by the alkaline transfer method (REF). The *T. cruzi* kDNA probe (kCR) was subjected to (α-^{32}P) -dATP labeling reaction with triphosphate deoxynucleotides dATP, dCTP, dGTP and dTTP (20 µM) described elsewhere. The reaction occurred for 3 h and the radio- labeled kCR probe was purified in a Sephadex G25 column. The membranes were then inserted into a cassette for film exposure to X- rays and stored at -80°C for 7 to 10 days. The films were washed with developing and fixation solutions in the dark to reveal the DNA bands.

Cloning and sequencing: The DNA sequences were determined after the third tpTAIL-PCR amplification cycle. Each mouse DNA of the *T. cruzi* integration sites into retrotransposon LINE families in the mouse genome. The primers employed in the reactions are shown in Table 4. sample was subdivided into eight aliquots. The amplification products from each tpTAIL-PCR third cycle from four repeat runs were ligated by T4 ligase into the pGEM T-easy vector at 4°C for 12 h. Competent Escherichia coli X10-Gold cells were treated with rubidium chloride and transformed by thermal shock. The cells were inoculated in Luria Bertani (LB) broth at 37°C for three hours to achieve maximal growth at OD 600. The broth was then centrifuged and the cells were transferred to a Petri dish to grow on LB agar with 4.8 × 10^{-2} µg/mL X-Gal and 0.1 µg/µL ampicillin [16-18].

Recombinant ampicillin-resistant white colonies that grew on nylon membranes were treated for hybridization with a radiolabeled kCR probe. The recombinants showing intense hybridization were selected for plasmid extraction. The inserts were released by EcoRI enzyme digestion and those showing strong hybridization signals were selected for commercial sequencing. Four rounds of the tpTAIL-PCR three- cycle amplification yielded selection of the nonredundant sequences from the DNA of each group of mice.

Sequence analysis: The sequences were analyzed for similarity with those from *Mus musculus* and *Trypanosoma cruzi* retrieved from the GenBank/NCBI. The non-redundant nucleotide searches were conducted throughout the GenBank/EMBL/DDBJ and RefSeqs databases. The Blastn version 2.2.25 parameters were e-threshold: 10 and word size 11. The threshold scores were match/mismatch 1, -2 gap costs, existence 5 and extension 2. The repeat masker CENSOR was used to map the sequences and the repeat classification was obtained by alignment with those in the LINE families A, T_F and G_F. The reference sequences L1Md-A2 (M13002.1) for family A, L1spa (AF016099.1) for family T_F and L1Md-GF62 (MG1:2178803) for family G_F [19].

Statistics: One-way ANOVA-F was employed for the statistical analysis and evaluation of the distributions of the kDNA mutations among the experimental data. Student's t-test was used to detect differences between uninfected control and kDNA mutated chicken progeny (FO to F2) and between kDNA mutation indexes in groups of *T. cruzi*-infected treated and untreated mice and the control uninfected groups.

Histopathology: The tissues from groups A to H mice were washed with 1X, PBS pH 7.2, fixed in 4% formaldehyde solution for 72 h., cut 5 µ thin sections and subjected to histopathological analysis.

RESULTS

Rabbit model

It has been observed that the treatment of chronically *T. cruzi*- infected humans with a trypanosome-killing agent neither stops the parasitemia nor the progressively destructive myocarditis and peripheral nerve system ganglions, hallmarks of Chagas disease. What could be sustaining the active destruction of the heart cells? To answer this question, it was postulated that a steady rate of genetic transfer could occur from the parasite to the host genome. The resulting mutation could explain

the autoimmune rejection of tissues of Chagas disease patients.

The ongoing process of genetic transfer between *T. cruzi* and rabbit was investigated by examining DNA from tissues extracted from eight rabbits that had been infected for six months to three years. BamH1 digests of DNA extracted from blood, heart, skeletal muscle, liver, intestine and kidney were hybridized with the kCR probe anneal to *T. cruzi* kDNA minicircle. A 2.2 kb band was obtained with the heart and intestine-derived DNA samples, distinct from the minicircle unit-sized 1.4 kb band hybridizing in parasite DNA alone. DNA extracted from tissues of uninfected rabbits showed no hybridization with the kCR probe. The tissue samples showed no hybridization with the other *T. cruzi*-specific nDNA probes for high-copy number genes repetitive sequences [20-23].

The PCR, cloning and sequencing showed large kDNA band sizes in the DNA of the heart and intestines, which are consistent with its integration in the genome. The *T. cruzi* infected and untreated (B) or treated with benznidazole (C) showed cardiomegaly and myocarditis, while the uninfected rabbit (A) showed none (5).

The experiments showed the integration of the kDNA minicircle sequence into a transposable element in the genome of a *T. cruzi*- infected rabbit. PCR amplification of rabbit DNA specific with primers S34/S35 and kCR kDNA probe. EcoR1 digested DNA (20 ug) separated in 0.7% agarose gel was used for southern hybridization with 1 ug of *T. cruzi* kinetoplast kCR probe. The *T. cruzi* DNA formed a 0.330 kb band of kDNA minicircle sequence. In contrast, the rabbit heart and intestine DNA yielded a 2.2 kb band, thus suggesting that the kDNA minicircle was integrated into the genome.

To characterize the 2.2 kb band, PCR with the kDNA direct and reverse primers was employed on DNA from infected rabbit hearts. This approach generated sequences containing both arms of rabbit DNA flanking the kDNA insertion (GenBank AY488498 to AY488503, AF399841, AF400668 and AF415293). Integration of a CCA/ACC rich kDNA fragment (bp 1255-1907) occurred at attachment sites of direct CACCAACC repeats within the rabbit DNA, thus indicating the kDNA minicircle sequence integrations were mediated by nonhomologous end-joining recombination [24,25].

The de novo transfer of kDNA to the rabbit genome occurred during the normal course of infection. The kDNA integration sites modified the human genome could represent a critical biological feature in host-pathogen interaction and clinical manifestation of Chagas disease.

Inoculation of purified kDNA sequences did not yield integrations of the exogenous minicircle into the rabbit genome.

***Trypanosoma cruzi* infection of rabbits, treatment with nitro- heterocycle benznidazole and pathology:** We performed experiments in groups of *T. cruzi*-infected rabbits to determine whether the administration of the benznidazole could halt the transfer of kDNA and Chagas heart disease pathology. Three groups of eight two-month- old male and female rabbits were housed in individual cages. The uninfected control group A rabbits were *T. cruzi* antibody-free. Figure shows the heart pathology in *T. cruzi*-infected rabbits. Panel A) Control, standard heart size (15 g) and histology from an 18- month-old New Zealand white rabbit. Panel B) Cardiomegaly (25 g) from a 15-month-old, *T. cruzi*-infected New Zealand white rabbit. Notice the cardiomyopathy with dilation of the right atrium and ventricle, as well as of the left ventricle. The histopathology showed mononuclear cell infiltration and lysis (minimal rejection units, arrows) of parasite-free target heart cells. Panel C) Cardiomegaly (30 g) from an 18-month-old *T. cruzi*-infected treated New Zealand white rabbit. Notice the cardiomyopathy with dilation of the right atrium and ventricle. The histopathology showed mononuclear cell infiltration and lysis of parasite-free heart cells [26].

The rabbits' groups B and C were each inoculated subcutaneously with 2.5×10^6 *T. cruzi* trypomastigotes. The drug powder (8 mg/ml suspension in 0.15 M saline) was administered to the *T. cruzi*-infected rabbits groups B and C (8 mg/kg body weight) during a period range from the 40^{th} day to the 100^{th} day post-infection. The *T. cruzi*- infected-untreated group B) and the *T. cruzi*-infected treated rabbits (group C) showed ELISA-specific antibodies throughout the long- lasting infections.

In the late chronic infection, groups B and C rabbits showed cyanosis, shortness of breath and ascites. The heart pathology of *T. cruzi*-infected rabbits either untreated (group B) or benznidazole- treated (group C) showed cardiomegaly with dilation of the atria and the ventricles. The histopathology revealed lymphocyte-lysed target cells. The severe myocarditis in the groups B rabbits was qualitatively like that seen in the benznidazole treated *T. cruzi*-infected group C rabbits. None of these lesions were seen in any tissue of control, uninfected rabbits.

Integration of *Trypanosoma cruzi* kDNA minicircle sequences into the rabbit and the chicken genomes: To continue the investigation of host-pathogen interactions in the rabbit, four sexually mature females and two males were crossbred during chronic infection. After three pregnancies, the does with chronic *T. cruzi* infections delivered 104 litters (26 ± 6 per doe). Three controls, uninfected females in three pregnancies delivered 96 litters (32 ± 3 per doe). PCR was carried out on

DNA from specific tissue of stillborn animals for both *T. cruzi* nDNA and kDNA. Evidence of genetic markers of the *T. cruzi* kDNA transfer. Specific hybridization of PCR amplification products from template DNA obtained from offspring of Chagas disease doe C using a set of *T. cruzi* kDNA specific primers. The EcoRI digested DNA products resolved in 1% agarose gels. PCR analysis of kDNA amplification showed bands of 300 bp and its customers from the parasite DNA and from the genomic DNA of six progeny with hybridization with the kCR probe [27].

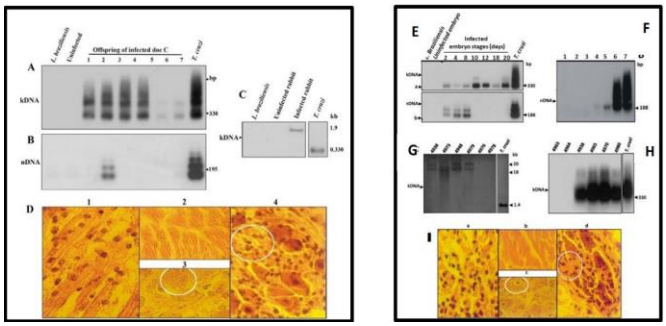

Figure 2: Genetic markers of *Trypanosoma cruzi* infection in offspring of Chagas disease rabbits (left) and chickens (right), kDNA transfer and pathology.

Hybridization of PCR amplification products from template DNA obtained from offspring of Chagas disease Doe C, using sets of *T. cruzi* nDNA and kDNA primers and specific radio-labeled nCR and kCR probes.

Left panel: A) Evidence of genetic markers of the *T. cruzi* kDNA transfer. Specific hybridization of PCR amplification products from template DNA obtained from offspring of Chagas disease doe C using a set of *T. cruzi* kDNA primers. The EcoRI digested DNA products resolved in 1% agarose gels. PCR analysis of kDNA amplification showed bands of 300 bp and its customers from the parasite DNA and the genomic DNA of six progeny with hybridization with the kCR probe. B) PCR analysis of nDNA amplification shows bands of 188 bp and its catamers formed with parasite DNA and from genomic DNA of offspring 2 after hybridization with the specific internal probe. This event suggested vertical transmission of the *T. cruzi* infection from Chagas rabbits' parents to the offspring 2 of Doe C [28-30].

Left panel: C) Southern hybridization shows the integration of kDNA minicircles into the offspring genome from a *T. cruzi* infected doe. Test and control DNA (20 ug) was digested with EcoRI and 10 ng of *T. cruzi* or *L. brasiliensis*. DNA for southern hybridization against the kCR probe. Separation of DNA products is achieved as described. The presence of the 1.9 kb band size higher than the minicircle 330 bp band indicated the integration of the kDNA into the rabbit genome. D) Representative myocarditis and lysis of target cells from kDNA positive kitten 1 of Doe C. 1) Histopathological section showing mononuclear cell infiltration and target heart cells. Note that the round lymphocytes adhere to the surface of the target cells and lysis. 2 and 3) Normal histological features of the myocardium and of intracardiac ganglion cell (white circle) from a control, noninfected kitten. 4) Intracardiac parasympathetic ganglion from a kDNA- positive kitten showing mononuclear cell infiltration and neuron dropout (circle).

The kDNA integration in germ line cells and bird tissues hatched from *T. cruzi* infected eggs, with accompanying pathology.

Panel E). A PCR analysis of nDNA amplification shows bands of 188 bp and catamers formed with parasite DNA and from genomic DNA of offspring two after hybridization with the specific internal probe. This event suggested vertical transmission of the *T. cruzi* infection from Chagas' parents to the offspring 2 of Doe C. F) Southern hybridization shows the integration of kDNA minicircles into the offspring genome from a *T. cruzi*-infected Doe. Test and control DNA (20 ug) was digested with EcoRI and 10 ng of *T. cruzi* or *L. brasiliensis*. DNA for southern hybridization against the kCR probe. The presence of the 1.9 kb band size higher than the minicircle 330 bp band indicated the integration of the kDNA into the rabbit genome [31-33].

F) Representative myocarditis and lysis of target cells from kDNA positive kitten 1 of Doe C. 1) Histopathological section showing mononuclear cell infiltration and target heart cells. Note that the round lymphocytes adhere to the surface of the target cells and lysis. 2 and 3) Normal histological features of the myocardium and intracardiac ganglion cell (white circle) from a control, noninfected kitten. 4) Intracardiac parasympathetic ganglion from a kDNA-positive kitten showing mononuclear cell infiltration and neuron dropout (circle).

A sample showing the presence of kDNA but not nDNA (offspring 1 of doe C) was examined by southern hybridization of EcoRI- digested genomic DNA with a kDNA probe. A band more southern hybridization of template DNAs from sperm and

from unfertilized eggs from experimentally infected rabbits retained the kDNA 330 bp bands in the genome. The control uninfected rabbit DNA showed no bands hybridizing with nDNA or kDNA probes. Out of the 104 surviving offspring from chronically infected parents, 24 (23%) contained kDNA, as determined by the PCR assay. Nine stillborn yielded DNA from the heart, skeletal muscle, liver, spleen and large and small intestine and each tissue type formed specific bands by hybridizing amplification products with a kCR probe.

This set of experiments demonstrated the vertical kDNA transfer to the genome of six progeny of the Chagas rabbit. In contrast, the transmission of the *T. cruzi* infection was documented in progeny 2, showing an upbeat DNA band. Although kitten 2 harbored the persistent infection, the progeny showing kDNA fragments in diverse tissue types suggested that some integrations occurred shortly after parasite invasion, thus resulting in the transfer of kDNA throughout the embryo germline cells. In addition, the results showed that *T. cruzi* infections in rabbits as well as in humans can be vertically transmitted from males and females to mates by intercourse.

These experiments showed that the de novo transfer of kDNA to the rabbit and chicken genomes is identical to its analog recognized in humans. Regarding the persistent *T. cruzi* infection in the benznidazole-treated rabbits, there was a concern about artifact parasite DNA contamination of tissues from an infected host. We tested the kDNA integration into chicken's refractory to *T. cruzi* infection to eliminate possible artifacts.

Chicken model system

To confirm and investigate the kDNA minicircle sequence integration into the vertebrate host's genome, we moved our studies to chickens, which are refractory to *T. cruzi* infection. The pathology documented in the tissues from kitten 1 of Doe C suggested that an early embryo *T. cruzi* infection could transfer the kDNA mini circle sequences in germline and somatic cells genome and therefore, the *ex vivo* uptake and invasion of the chicken blastula stage embryo stem cells was first explored. The kinetics of the *T. cruzi* infections in fertile chicken eggs inoculated with 100 *T. cruzi* trypomastigotes before incubating at 37°C were documented. On the eighth day of incubation, the embryo stem cells with the dividing amastigotes were identified by a fluorescein-labeled anti-*T. cruzi* antibody and X-Gal staining. Using this immunohistochemical approach, we confirmed amastigotes of *T. cruzi* in chicken embryo endoderm and mesoderm tissues at embryonic stages 4 and 8 days old. The *T. cruzi* amastigotes in the embryo stem cells examined by electron microscopy showed a typical disc-shaped kDNA network and membrane wrapped around the DNA nucleus.

The permissiveness of embryonic stem cells to a *T. cruzi* infection of a 2-day-old zygote at the blastula stage was an indication of differentiating germline cells in the genital crest, which appear at days 4-8.5 of gestation. Thus, germ line cells could encroach parasite-27 host cell interactions, displaying early drug inhibitor effect on cell growth and prevention of kDNA transfer. In control experiments, we inoculated naked minicircle or cloned minicircle sequences in the air chamber of 30 fertile chicken eggs. The absence of PCR amplification products from these embryo's template DNAs tested weekly prior to hatching indicated that, as in rabbits, transfer of minicircle kDNA sequences to a bird's genome requires a living infection.

Thirty-six fertile chicken eggs were each injected with 100 *T. cruzi* trypomastigotes. The embryo tissue collected on the second, fourth and eighth days of infection yielded nDNA and kDNA amplification products; however, tissue collected on the tenth, 12th, 18th and 20th days of incubation, yielded amplification products only for kDNA, indicative of the clearance of the active infection. The experiments in the chicken model system were focused on the dissociation of kDNA integration from cryptic *T. cruzi* infection. Therefore, a kDNA integration event early in embryonic development could generate a sexually mature chicken with kDNA integrated into gonadal tissue.

To confirm the refractoriness of chickens to *T. cruzi* infections, we employed a PCR assay with the Tcz1/Tcz2 primers and hybridization of amplicons with the radiolabeled 188-bp nDNA probe. These experiments revealed that the sensitivity of the PCR assay (10 fg) was much fold below the level of a diploid parasite (240 fg) nDNA and therefore, the eradication of *T. cruzi* infections from the chicken body was no longer an issue. These results validate the findings of kDNA minicircle sequence integration into germline and somatic cells. Furthermore, the presence of kDNA with mobility differential from minicircles in the gonadal DNA of individual chickens combined with the absence of *T. cruzi* nDNA attested to the integration event's success and the subsequent eradication of *T. cruzi*.

To determine whether kDNA-transfected birds harbored *T. cruzi* specific DNA in germline cells, we collected sperm from 4938 and 4965 and eggs at an early stage of 28 developments from the ovaries of hens 4970 and 4980. DNA templates extracted from these samples yielded kDNA but not nDNA amplification DNA from tests and ovaries of control, uninfected birds 4963 and 4964 did not produce products [34].

To determine whether kDNA-transfected birds harbored *T. cruzi* specific DNA in germline cells, we collected sperm from

4938 and 4965 and eggs at an early stage of 28 developments from the ovaries of hens 4970 and 4980. DNA templates extracted from these samples yielded kDNA but not nDNA amplification DNA from tests and ovaries of control, uninfected birds 4963 and 4964 did not produce products.

Germline transmission of integrated kDNA in Gallus gallus: We examined the transmission of integrated kDNA to the resulting progeny chicken independent of persistent or cryptic *T. cruzi* infection. The kDNA-transfected rooster 4938 and hens 4973 and 4948 were bred to produce vertical, germline transmission of kDNA to their offspring. Twelve chicks born from these crosses carried kDNA in their genomes, as shown by amplification from blood cell DNA. The kDNA-positive f1 birds then crossed to obtain f2 hybrids, producing lineages of kDNA transfected progeny. kDNA transfected rooster 4979 and control, uninfected hens 4976 and 4978 were bred to detect the frequency of vertical inheritance of kDNA to F1 and F2 offspring from a single kDNA donor parent. All chicks born from these crosses showed kDNA in their genomes, thus indicating that integrated kDNA can be inherited through the male. Cloning and sequencing revealed kDNA (GenBank 531591 to 531759) integrated into the chicken genome. In a control PCR for nDNA, no bands were obtained from any offspring DNA samples. These results validated the vertical transfer of *T. cruzi* kDNA into the chicken genome.

The tpTail-PCR amplification products, cloning and sequence analyses revealed that transposable elements hitchhiked the mitochondrion kDNA-minicircle sequences into the gene encoding a cell surface glycoprotein-derived neurotrophic receptor (FN 598975) at chromosome 13 and into the alpha three genes encoding a glycosylphosphatidylinositol cell surface receptor. In addition, samples of the kDNA mutations (FN 598 972 and FN 598982) into coding regions of serine/threonine protein kinases and phosphatases, playing roles in signaling and adaptation to environments, were found in chromosome 14. Furthermore, the kDNA mutations (HG531472) inserted at the Dystrophin gene, encoding an associated protein complex, scaffold various signaling proteins at chromosome 1. The GenBank data with further kDNA mutations, showing gene reshuffling and remodeling at several chromosomes, are displayed.

In this study, separating the kDNA minicircle sequence integration event from active infection with *T. cruzi* indicates that our observations are valid. With this respect, the functional consequences of the kDNA integration sequence were sought at bone marrow cells, progenitors of effector cells, causing autoimmune myocarditis and Chagas disease.

Chagas-like clinical and pathological manifestations in chickens: The kDNA-mutated chickens developed clinical symptoms like those of rabbits and humans with Chagas disease. The $kDNA^+$ and the healthy $kDNA^-$ chickens were inspected weekly. Signs of shortness of breath were observed in the $kDNA^+$ chickens and cyanosis, ascites and pleural effusions were constant ominous signals of heart failure in the kDNA-mutated group of chickens. The ECGs recorded at three and six months in 12 F0 kDNA mutated chickens and 22 kDNA-negative controls showed the test birds changed the axis position to the left from +80° to -115° over time, whereas the controls retained the electric axis at +75°. Ascites and pleural effusions were collected in kDNA-mutated birds with heart failure [35].

The parasite-free-pathology-translated clinical findings in chickens hatched from the *T. cruzi* infected egg showed kDNA mutations in chromosomes 2 and 13.

Left panel: A) Nine-month-old chicken with heart insufficiency, cyanosis (left) and a control hen of the same age showing a bright red comb. B) ECG alteration with a shift of cardiac axis from a-to-c over six months. C) The body heart weight indexes showed statistically significant differences ($p<0.05$ in control and kDNA-mutated chickens. D) cardiomegaly (30 g) in a nine-month-old hen that died of heart failure. E) Control heart (15 g) from a nine-month-old hen. F) Diffuse myocarditis showing cytotoxic lymphocyte infiltrates and lysis of target heart cells. The red cycles depict minimum rejection units where several lymphocytes lysis a target cell. G) Normal myocardium histology of an adult hen. H) kDNA-mutated chicken, intracardiac parasympathetic ganglion showing mononuclear cell infiltrates and neuronal cell lysis; I) Control, normal histology of an intracardiac ganglion.

J) Lack of B cell after treatment with anti-Bu-1 monoclonal antibody.
K) CD45+ lymphocytes identified (arrows) in heart lesions by a phycoerythrin-labeled specific monoclonal antibody. L) CD8+γδ immune lymphocytes (arrows) are involved in severe destruction of the heart. M) Abundant CD*α+ T cells in severe lesions with heart cell lysis. N) Monocytes and macrophages in the heart lesions.

The kDNA-mutated chickens' heart body weight indexes ranged from 6 ± 2 to 6.7 ± 2 and 12 ± 5. The index in the control chicken group was constant at 4.2 ± 2. We documented statistically significant differences among the high heart size indexes from F0 and F1 kDNA mutated chickens from those low indexes from controls ($p<0.05$ Consistently, survival length for those groups of kDNA-mutated chickens was shorter for F0 (12 ± 4 months) and F1 (13 ± 2 months) than those in the control group (19 ± 5 months). These differences are statistically significant ($p<0.05$).

The gross pathology in birds hatched from *T. cruzi* infected eggs consisted of cardiomegaly like that seen in human Chagas disease. The chickens' hearts showed thickening of the walls of the ventricles and dilation of the chambers. Control, healthy chickens showed standard heart size. In these experiments, the histopathological analysis of the myocardium showed the destruction of parasite-free heart cells by effector mononuclear cells. It depicted the hallmark rejection of the target cell, characterizing minimal rejection units (red circles) in the myocardium. The control sections of the myocardium showed normal histology.

The finding of the parasite in the heart was unexpected because the chicken's innate immunity eradicates *T. cruzi* infection. Ganglionitis with lysis of target cells, but these features were not observed in the control parasympathetic neurons. Those inflammatory infiltrates reached the wall of the intestines and skeletal muscles. The antibody- producing B-lymphocyte was absent in those inflammatory infiltrates. However, the immunohistochemical assays of myocardium from kDNA-mutated chickens treated with anti-CD45, anti-CD8γδ or with CD8α and macrophages treated with MPS antibody showed specific staining of these lymphocytes carrying out lysis of target heart cells. In control experiments, the sections from the myocardium of control chickens (inserts) showed neither cytotoxic lymphocytes nor tissue destruction markers.

Chickens with a mutation in the dystrophin gene (GenBank sequence mutation RG531472) showed myocarditis with inflammatory cell infiltrates in the heart and skeletal muscles and severe lysis. The parasympathetic nervous system also showed lymphocyte infiltrates and neuronal cell lysis. Myocarditis, myositis and ganglionitis in a rooster with a kDNA minicircle sequence mutation (RG531472) in the dystrophin gene. Control chickens showed standard histology (inserts).

These findings show that insertions of kDNA minicircle sequences in transposable elements could hitchhike to several coding regions in the chicken genome, thus initiating autoimmune rejection of body tissues over time. Given these results, we investigated whether the multidrug treatment of *T. cruzi* infection with the lead compound benznidazole in combination with drug inhibitors could prevent eukaryote cell division and growth *ex vivo* and inhibit the kDNA transfer.

Searching for drug inhibitors of *T. cruzi* kDNA transfer:

The selected array of inhibitors of eukaryote cell growth was aimed at the multidrug treatment of *T. cruzi* infections with specific objectives: i) lethal effect against the *7 FUX]L* forms; ii) minimal toxicity to the host cell; iii) abolishment of kDNA transfer. The optimal concentration of metabolic pathway inhibitors was determined by the *LQ YLWUR* dose- response. The better inhibitors were selected in triplicate *H[YLYR* experiments using different drug concentrations. The optimal dose was determined for *7 FUX]L* epimastigote (10×10^6/mL) incubated for four h at 27°C with each drug at a concentration two times above and two times below the optimal dose. After that incubation, the cells were transferred to culture tubes containing agar slants with LIT medium overlay. Three repeat experiments were conducted to determine the drug concentration-killing effect in aliquots of specific inhibitor treated T. cruzi forms suspended in fresh LIT medium and grown in a shaker incubator at 27°C for 8 days. The motile epimastigotes showing typical whitish silhouettes in a counting chamber, which were recorded and plotted and the cytotoxic effect of each drug inhibitorwas determined. The drug concentration that killed 75% and above the T. cruzi epimastigotes in LIT medium for one week was chosen.

The experiments further assessed the drug inhibitor toxicity against L6 muscle cells. A 10×10^5/mL muscle cell suspension in DMEM was incubated with the optimal inhibitor concentration. Three independent repeat experiments were performed for each of the twelve drug inhibitors. The mock control *T. cruzi* infected muscle cell suspension was maintained without the drug inhibitors. After 14 days of incubation, the muscle cell monolayers were washed with PBS, stained with H-E and examined.

The moderate and severe toxicity of the inhibitors on the target cells revealed the blurred fade-away silhouette of some amastigotes. In contrast, the muscle cells lost membrane boundaries and cytoplasm vacuolation. None of these features were seen in the cells without a drug inhibitor. These experiments revealed severe toxicity of microcystin, bromodeoxyuridine and mitomycin in muscle cells. Cycloheximide, staurosporine, genistein, etoposide and camptothecin showed moderate toxicity and praziquantel showed mild toxicity. Ofloxacin and Azidothymidine, which killed the *T. cruzi* epimastigotes, did not destroy the L6 muscle cells; therefore, they were selected for *in vivo* experiments in the mice models.

T. cruzi infected macrophage cocultures and DNA assessment: The parasite persistence within a mammalian is hidden from the host immune system inside nonphagocytic cells. Because the integration of *T. cruzi* minicircle kDNA sequences into the macrophage genome would cause host cell-pathogen interactions, this phenomenon was investigated *ex vivo*. Having identified the dose of each inhibitor that did not kill muscle cells, we investigated the effect of the drug- mediated inhibition of kDNA transfer to the genome of *T. cruzi* infected human macrophages. The southern blot analysis of the *T. cruzi* infected macrophage DNA-PCR amplification products obtained with specific primer sets and radio-labeled kCR probe showed that the

phosphorylases, polymerase II and late phase cell division inhibitors: Mitomycin, cycloheximide, etoposide, genistein, ofloxacin, praziquantel and staurosporine, prevented the formation of the large 1.2, 1.8 and 2.2 kb kDNA minicircle sequence bands. In addition, colchicine, which suppresses tubulin assembly and microtubule formation and azidothymidine, which intercalates thymidine to DNA, inhibiting reverse transcriptase and telomerase at the G2/M cell growth phase, abrogated the transfer of large 1.2, 1.8 and 2.2 kb kDNA sequence bands [36].

Panel A. *Trypanosoma cruzi* macrophage cocultures and DNA assessment on day 21st post-treatment with cell growth and development inhibitors. The PCR amplification products were separated in a 0.7% agarose gel, blotted and probed with the radiolabeled kCR probe for the conserved minicircle sequence. The results are representative of three repeat experiments. Note that the microcystin concentration that killed *T. cruzi* and prevented 0.330 kb band formation did not inhibit the integration of the kDNA band, forming the upper 2.2 kb band. In contrast, bromodeoxyuridine and campthothecin did not abrogate kDNA bands. The other inhibitors prevented large 1.2, 1.8 and 2.2 kDNA bands but they did not inhibit the 0.330 kb band formation. The positive control *T. cruzi* kDNA formed a typical 0.330 kDNA band and the control DNA showed no band.

In contrast, microcystin, camptothecin and bromodeoxyuridine, respectively, inhibitors of phosphatases and polymerase I, that form DNA adducts at phase S cell cycle, did not inhibit the transfer of the 1.2, 1.8 and 2.2 kb bands into the host cell. Interestingly, microcystin, a serine/threonine phosphatase PP1 and PP2A inhibitor, inhibited the formation of the 0.330 kb kDNA band only. The PCR amplification of the purified *T. cruzi* kDNA showed a single 330 bp band only, whereas the *T. cruzi* infected macrophage DNA yielded the 330 bp band and in addition, it formed 1.2, 1.8 and 2.2 kb kDNA bands. The control macrophage DNA showed no band.

The macrophages were collected on day 21 post-infection with *T. cruzi* and treated with the inhibitor concentration. The DNA-PCR amplification products hybridized with the radio-labeled kCR minicircle probe revealed that phosphorylases, polymerases and late- phase cell division inhibitors precluded the transfer of the 1.2, 1.8 and 2.2 kb kDNA bands into the macrophage genome. Microcystin, camptothecin and bromodeoxyuridine did not prevent the transfer of the sequences detected at high molecular weight bands. Microcystin prevented the formation of a 0.330 kb kDNA band. The modification of band profiles indicated that kDNA minicircle sequences transfer into the host cell genome, representing a persistent element in host-pathogen interactions. The persistence of the kDNA upper band sequences in the macrophage genome was observed over several years and the cells were maintained in tissue culture. In this respect, we searched for drug inhibitors of the phenomenon of *T. cruzi* kDNA transfer into the host cell genome.

Mouse models

Multidrug treatment of *T. cruzi* infections: To confirm and dissect the effect of the drug inhibitors on eukaryote cell growth, we moved our studies into the mouse model system, which shows a short lifespan and is sensitive to *T. cruzi* infection. The evidence of kDNA integration into the macrophage genome led us to anticipate a therapeutic regimen encompassing the combination of drug inhibitors with the lead benznidazole to treat Chagas disease. On the one hand, we used azidothymidine, which intercalates thymidine to inhibit reverse transcription and apoptosis. On the other hand, ofloxacin 4- fluoroquinolone inhibits the polymerase metabolic pathway at the G2/M phase and apoptosis. In addition, the praziquantel quinolone derivative enantiomer was administered to *T. cruzi* infected mice. This experiment aimed to determine whether the multidrug treatment that curtailed the infection would prevent the lateral transfer of kDNA integration into the mouse genome and associated pathology. Groups of eight mice each were inoculated with the *T. cruzi* trypomastigotes (2×10^3) intraperitoneal and multidrug treatment regime by gavage initiated at the 5th-day post-infection; the *T. cruzi* infected untreated was the positive control group.

The results of these experiments showed that independent administration of either benznidazole, azidothymidine, ofloxacin or praziquantel to treat each of eight acutely *T. cruzi* infected BALB/c mice curtailed the presence of the protozoan flagellates in the blood from 40 to 20 days.

The peak of parasitemia was detected in *T. cruzi* infected and untreated mice at 40 days of infection. A quick fall was observed in the *T. cruzi* infected groups of mice treated with either benznidazole, azidothymidine or ofloxacin, clearing tail blood (5 uL) parasitemia on day 20. Parasitemia lasted for 20 days in the *T. cruzi* infected mice treated with a combination of benznidazole-ofloxacin or benznidazole- azidothymidine. The results further showed the parasitemia abbreviated to 15 days in the group of mice treated with benznidazole, azidothymidine and ofloxacin. However, the blood cultures set at the 20th, the 40th and 60th day post infections yielded *T. cruzi* species.

Panel C. Southern hybridization of *T. cruzi* kDNA-PCR product form Mus musculus subjected to a multidrug therapeutic

regime. The solid tissues from each group of mice (n=8) were minced with sterile blades and the tissue was subjected to DNA extraction and purification. The PCR amplification products were analyzed in agarose gel electrophoresis, blotting and southern hybridization with a radio-labeled kCR probe. Note the 330 bp kDNA band in groups of *T. cruzi* infected mice: i) untreated; ii) benznidazole-treated; iii) benznidazole, azidothymidine and ofloxacin treated. B, blank; C1 and C2, uninfected controls; *T. cruzi*, positive control.

The evidence of toxicity prevented the administration of praziquantel in other mouse groups. In addition, the experiments showed that further abolishment of the flagellates in the blood was achieved with the two-by-two combination of benznidazole with azidothymidine and with benznidazole and ofloxacin: The employment of the lead nitro heterocyclic compound in combination with azidothymidine and ofloxacin, inducers of cell growth inhibition and apoptosis, curtailed parasitemia from 40 to 15 days. On the 250th day postinfection, the mice of all groups were sacrificed under anesthesia and the tissues were collected by necropsy. The body tissue samples were minced and processed for DNA purification and analysis. The persistence of the *T. cruzi* infections in the mice of each group was demonstrated further by PCR amplification with nDNA- specific primer sets and with southern blotting hybridization.

Given the curtailment of parasitemia and abrogation of the 330 bp kDNA band in the *ex vivo* macrophage assay, we ran experiments to assess the effect of the multidrug treatment on preventing the integration of kDNA minicircle sequences into the mouse genome.

The ofloxacin and praziquantel piperazine derivative enantiomers inhibited *T. cruzi* growth *in vitro*. However, the mild cytotoxicity of praziquantel against murine muscle cells suggested its exclusion from the therapeutic regimen given to the *T. cruzi* infected mice. In this regard, we continued the experiments assessing the inhibition of the lateral transfer of the kDNA minicircle sequence to the Chagas disease mouse genome.

The results of the *T. cruzi* kDNA PCR-amplification with the S35/S36 primers, separation of the products in a 0.8%agarose gel, blotting and radio labeling with the radiolabeled specific kCR probe. This qualitative PCR technique is direct evidence of some 330 bp kDNA minicircle sequences integrated into the genome of the *T. cruzi* infected mice treated with the lead multidrug therapeutic regimen.

In previous experiments, we showed kDNA minicircle sequence integration into the genomes of *T. cruzi* infected rabbits and chickens hatched from the *T. cruzi* inoculated eggs.

The tpTAIL-PCR techniques with the specific primer sets revealed the leading site of the kDNA minicircle sequence integration into the rabbit (LBNL-1) and chicken (CR-1) LINE-1 retrotransposons on several chromosomes. Moreover, we showed that 70.8% of the *T. cruzi* kDNA integrations were observed in retrotransposons LINE-1 into the human genome (EMBL HG008116 to HG008708). The schematic representation of the qualitative tpTAILPCR employed to disclose the kDNA mutations in the *Mus musculus* genome was shown in a previous paper. The procedure included the uninfected mouse DNA and *T. cruz*i DNA internal controls and the last cycle of the tpTAIL- PCR showed the host *T. cruzi* DNA chimeras only.

The A/C rich nucleotide microhomologies at the site of integration in the mouse DNA and in the kDNA minicircle constant sequence repeats intermediated nonhomologous endjoining recombination and lateral transfer of the *T. cruzi* mitochondrial minicircle sequence. The quantitative nucleotide searches proceeded throughout the GenBank/EMBL/DDBJ and Refseqs database. The masker CENSOR was used and the redundant sequences were excluded by alignment with those in the mouse LINE families.

In these experiments, mixed tissue DNA from each mouse was subjected to four independent repeat triplicate samplings of tpTAIL- PCR and the average nonredundant hybrid sequences obtained from each of the five experimental groups of mice. A) Schematic representation of the average kDNA transfer in *T. cruzi* infected groups of mice treated with lead compound benznidazole in combination with azidothymidine and ofloxacin. The average nonredundant kDNA transfer into each *T. cruzi* infected mouse group (n=8) revealed the following: Group I, untreated, 4.9 ±2.6; group II, treated with benznidazole, 5.2 ± 2.7; group III, treated with benznidazole+azidothymidine, 6 ± 2.4; group IV, treated with benznidazole+ofloxacin, 3.4 ± 0.9; group V, treated with benznidazole +azidothymidine+ofloxacin, 2.0 ± 0.4. This last group of kDNA mutations showed statistically significant differences ($p<0.05$) in the mice group I to III. This result is 2.44-fold below the total number of mutations compared to those disclosed in the genome of *T. cruzi* infected, untreated mice.

The hybrid sequences with an average size of 505 ± 260 nucleotides are displayed in Table 4. The data revealed that 79% of the lateral transfers of the kDNA minicircle nonredundant sequences took place at Family A, LINE-1 into the genome of the *T. cruzi* infected mice. The control group of mice showed standard heart size and histology. However, the pathology study

revealed that the *T. cruzi* infected mice treated with benznidazole+azidothymidine+ofloxacin showed evanescent myocarditis and discrete fibrous tissue fibers in the myocardium. These features stemming from the multidrug treatment correlated with a threefold decrease in the ratio of kDNA integrations in the mice receiving benznidazole+azidothymidine+ofloxacin.

The uninfected, control adult mouse heart size. C) Normal heart histology of a control, uninfected mouse. D) Dilated cardiomyopathy of a benznidazole-treated Chagas' mouse. D) Inflammatory autoimmune rejection and the destructive myocarditis with lysis of the target heart cells (minimal rejection unit, asterisks) in a chronically *T. cruzi* infected mouse in the absence of amastigote nests *in situ*. E) Myocarditis of a mouse is treated with benznidazole and azidothymidine. F) Similar myocarditis was seen in a mouse treated with benznidazole and ofloxacin. G) Quenching myocarditis in a mouse treated with a cocktail of benznidazole+azidothymidine +ofloxacin. Notice that the representative histopathological findings in mouse group H is in keeping with lowered kDNA integrations into the genome.

Severe cardiomegaly and intense heart cell lysis were present in the T. cruzi infecteduntreated mice myocarditis. Myocarditis and heart cell lysis were observed in the mice groups reduced myocarditis and target heart cell lysis were documented in rabbits that received benznidazole +ofloxacin+azidothymidine.

DISCUSSION

In this study, the employment of cross-kingdom animal models showed that the chickens refractory to the *T. cruzi* infection retained the kDNA minicircle sequences integrations into the genome and developed the typical myocarditis of Chagas disease. The clinical- pathological manifestations of the disease were also documented in chicken refractory to the *T. cruzi* infections. The absence of *T. cruzi* nDNA in chickens hatched from eggs inoculated with the flagellates substantiates the cardiomegaly in the kDNA-positive chicken contrasted with the small heart size of the kDNA-negative control chicken. The myocarditis documented in the kDNA-positive chickens hatched from *T. cruzi* infected eggs was identical to that of Chagas disease in humans, rabbits and mice. The microscopic analysis of the myocardium revealed severe infiltrates of lymphocytes and target cell lysis. These microscopic features were absent in the heart of kDNA- negative control chickens.

Contrastingly, the pathology of Chagas disease has not been reproduced in a suitable animal model challenged with any molecular predictors of myocardiopathy. Chagas-like cardiomyopathy is produced in the chicken model system, which naturally eliminates the parasite and retains the kDNA minicircle sequence mutations in the genome. The direct evidence of kDNA minicircle sequence mutations and Chagas cardiomyopathy is documented in the parasite-free chicken model, showing the rejection of self-heart cells by immune T- lymphocytes. Therefore, the kDNA mutations in the hosts' genome are a genuine biomarker for monitoring the efficacy of multidrug treatment of Chagas disease.

We reproduced heart disease in the rabbit model infection system that developed Chagas disease, indistinguishable from that described in humans. The active process of genetic transfer between *T. cruzi* and rabbits was initiated by examining the effect of lead benznidazole in treating Chagas disease. With this respect, a treatment strategy compatible with disease pathogenesis was hypothesized. For the lack of irreversible drug elimination of the *T. cruzi* infection, we sought to curtail the parasitic load and to lower the accumulation of the kDNA minicircle sequences integrating into the host's genome, therefore reducing polygenic modifications that could exacerbate the parasite- induced, genetically driven autoimmune mechanism lethal to approximately one-third of the Chagas disease patients. The hypothesis addressed the autoimmune rejection of self-tissue inhibition by multidrug treatment of Chagas heart disease and prevention of *T. cruzi* kDNA minicircle sequence integration into host cells genome. We tested various drug inhibitors of eukaryote somatic and germ-line cell metabolic pathway checkpoints. The optimal concentration of 12 drug inhibitors was tested *in vitro* against the *T. cruzi* forms. Three independent replicate experiments revealed the growth inhibitory efficacy of bromodeoxyuridine, azidothymidine, ofloxacin and praziquantel. To determine the cytotoxicity of the array of 12 inhibitors, we incubated each drug with monolayers of *T. cruzi* infected L6 murine muscle cells fed culture medium at 37°C in a 5% CO_2 incubator. The results showed the severe cytotoxicity of microcystin phosphatases inhibitor mitomycin and bromodeoxyuridine, which is a cross-linker that forms DNA adduct by covalent attachment to target macromolecules. The severe cytotoxicity against the eukaryotic cells observed under the microscope consisted of loss of the cell membrane boundaries, foamy cytoplasm formation and death. It was observed that the inhibitor microcystin hold blocked the formation of the 0.330 kb band. Still, it did not prevent the integration of the upper 1.2, 1.8 and 2.2 kb kDNA minicircle sequence bands into the macrophage genome, unlike camptothecin and bromodeoxyuridine, which did not prevent the formation of any of those bands. Nevertheless, the microcystin serine/ threonine protein phosphatase inhibitor induced cell death should undergo further

study toward developing a new drug to kill the *T. cruzi* agent of Chagas disease. An independent assay that searched for the integration of *T. cruzi* kDNA minicircle sequences into the human macrophage genome showed an array of polymerase inhibitors of eukaryotic cell division prevented the transfer of the minicircle sequences and elimination of the 1.2, 1.8 and 2.2 kb bands, which was different from the situation of the 0.330 kb mitochondrial kDNA band. To approach the multidrug treatment of *T. cruzi* infections, we selected the polymerases inhibitor 4-fluoroquinolone and ofloxacin the azidothymidine reverse transcriptase inhibitor and the lead nitro heterocycle benznidazole.

The treatment of the acutely *T. cruzi* infected BALB/c mice with benznidazole curtailed parasitemia at the 20th day of the drug administration. In contrast, the flagellates lasted for 40 days in the blood of the infected-untreated mice. Additionally, hemoculture, the ELISA for specific antibodies and the *T. cruzi* nuclear DNA- PCR consistently yielded positive results for *T. cruzi* infected mice that had received the dose of benznidazole used to treat the infection. Two out of eight mice each in the *T. cruzi* infected-untreated and in the infected-treated groups developed identical Chagas heart disease and died with dilated cardiomegaly due to severe myocarditis. This caveat shows that the administration of benznidazole to treat *T. cruz*i infection is unsatisfactory. The information is in keeping with the observations stemming from experimental protocols in animal models and, accordingly, with the data obtained from *T. cruzi* infected treated rabbits and human Chagas disease clinical trials.

Insights into human Chagas disease: Comparative pathology experiments carried out in chicken's refractory to *T. cruzi* and in rabbits amenable to infection revealed that the pathogenesis of Chagas disease stems from clones of kDNA mutated lymphocytes, which rejected target heart cells. In this regard, we sought to reproduce the phenomenon in the rabbit model infection system that developed Chagas disease, which is indistinguishable from that described in humans. The active process of genetic transfer between *T. cruzi* and rabbits was initiated by examining the effect of a lead benznidazole in treating Chagas disease. In addition, the production of Chagas heart disease in chicken's refractory to *T. cruzi* infection and mice susceptible to persistent parasite infection was essential to demonstrate that lateral kDNA transfer triggers the pathogenesis of the disease.

This study aimed to prevent the transfer of kDNA into the host´s genome by administering a multidrug cocktail of inhibitors of the central metabolic pathway checkpoints of cell growth and differentiation. First, it was found that treating chronically *T. cruzi* infected mice with a cocktail of benznidazole with azidothymidine and ofloxacin produced a 2.44-fold decrease in kDNA mutations in the mouse genome. Accordingly, we documented that the mice in this multidrug-treated group had reduced severe myocarditis compared with those in the *T. cruzi* infected and benznidazole treated group.

The vertebrate genome contains various copies of retro- transposable elements. Humans have approximately 400 copies of active LINEs belonging to different subsets, whereas mice contain over 3,000 copies belonging to various family and type subsets. These elements are likely progenitors of *T. cruzi* mutagenic insertions, providers of means for mobilization and reshuffling of DNA sequences around the genome and Chagas disease over time.

Integrating the protozoan kDNA minicircle sequence into the germline of chicken and mouse cells' LINEs and SINEs transposable elements at several chromosomes usually produced neutral mutation and positive selection. However, we observed that minicircle sequences hitchhiking and kDNA sequence mobilization to coding regions, creation of new genes and pseudogenes and silencing of genes may produce polygenic alterations and the genetic mechanism of disease. The sheer number of minicircles, each with four conserved regions containing CA-rich repeat sequence motifs, could be the dominant characteristic influencing the high frequency of these serendipitous mutagenic events that influence endogenous host genes and Chagas heart disease over time. The transposable elements replicated within the host genome may contribute to somatic mosaicism; thus, potent regulatory polygenic modifications in the diseased state play a role in the pathogenesis of inflammatory autoimmune disease. In this regard, Chagas heart disease could stem from the mutation-induced genome modification and the onset of surreptitious alterations contributing to the activation of CD45, CD8+ and CD8ɣð+ effector cells that express vß1 and v ß2 receptors involved in target cell rejection [37].

The kDNA insertion mutations underpinning alterations of the effector and the target host's cells undergo polygenic modifications stemming from LINE-1 elements intermediate genome reshuffling, forming *T. cruzi* induced autoimmune-driven lesions. The threatening heart disease exacerbation in approximately one-third of chronically infected individuals results in a short survival of two to five years. The timely investigation of those Chagas heart disease cases revealed an accumulation of lateral transfer of the kDNA mutation range from a minimum of 4 to 8 into the LINEs located on various chromosomes.

The refractoriness of avian to the *T. cruzi* flagellate protozoan was convenient for this study. It aimed to inhibit autoimmune Chagas heart pathology because it did not require pre-cleaning of the infection. Thus, each kDNA-integrated

mononuclear immune cell involved in the "self" tissue destruction is essentially a mutated clone homing to the target organ where the cytotoxic lymphocyte promotes the lysis of the target cells. Alternatively, in the absence of deleterious polygenic alteration and modification, this hypothesis could explain the long- lasting asymptomatic infection of a significant parcel of *T. cruzi* infected population and in some patients with mutagenic kDNA fragments dispersal by active LINE-1 mobilization within the genome undergoing occasional reversal of symptoms.

Homing and organ specificity: Homing of the bone marrow derived kDNA-mutated lymphocytes toward the target counterpart cells was observed. Second, the organ specificity of the muscle and the parasympathetic neuronal cell targets of genetically driven autoimmune rejection were informative. We suggest that selective effector-target cell signaling affinity could be a genetically acquired trait dependent upon the *T. cruzi* kDNA-integrated minicircle, showing interspersed constant and variable CSB1, CSB2 and CSB3 possible intermediates of kDNA transfer to hundreds of homologous, average 8 to 25 nucleotides share into the human genome. Additionally, we hypothesize the share repeats, folding and loop forming tri-dimensional structures, binding sites for positive and negatively charged protein electron emission signaling pathway and closed lock selection of the target for the autoimmune tissue rejection. The specificity of the target organ rejection now, called out through stoichiometry change repeats thus, DNA folding and loop tri- dimensional structures, selective sites of charged proteins binding sources of a cell-to-cell signaling pathway, homing and organ selection. The signaling pathway studies of chromosome skewing and instability-generated interactions could substantiate the organ specificity and homing, genetically driven disease mechanism ensuing rupture of immune tolerance and its eventual attenuation due to chromosome upright remodeling. We suggest that groups of kDNA minicircle sequence integration mutations, polygenic modifications and alterations may explain lymphocyte toxicity and rejection of the target host's cells in Chagas disease.

This study showed that treating *T. cruzi* infected mice with benznidazole, azidothymidine and ofloxacin lowered the kDNA minicircle sequence integrations and reduced the rejection of target heart cells and Chagas disease. These drugs are FDA-approved for human use.

CONCLUSION

In conclusion, the histopathology showed that the benznidazole +azidothymidine+ofloxacin therapeutic regime prevented the myocarditis and reduced the target cell lysis, which is a hallmark of autoimmune Chagas cardiomyopathy, in the absence of the parasite *in situ*.

ETHICS STATEMENT

The human and the animal research committees of the faculty of 50 medicine of the University of Brasilia approved all the procedures with human subjects and laboratory animals research protocols 2500.167567 and 054/09, respectively. The laboratory animals received humane care; the mice under anesthesia were subjected to heart puncture before sacrifice.

REFERENCES

1) Klein N, Hurwitz I, Durvasula R (2012) Globalization of Chagas disease: A growing concern in nonendemic countries. Epidemiol Res Int 2012:136793.
2) Lidani KC, Andrade FA, Bavia L, Damasceno FS, Beltrame MH, et al. (2019) Chagas disease: From discovery to a worldwide health problem. Public Health Front 7:166.
3) Herreros-Cabello A, Callejas-Hernandez F, Girones N, Fresno M (2020) *Trypanosoma cruzi* genome: Organization, multi-gene families, transcription and biological implications. Genes 11:1196.
4) Callejas-Hernandez F, Herreros-Cabello A, del Moral-Salmoral J, Fresno M, Girones N (2021) The complete mitochondrial DNA of *Trypanosoma cruzi:* Maxicircles and minicircles. Front Cell Infect Microbiol 11:672448.
5) Coura JR, Dias JC (2009) Epidemiology, control and surveillance of Chagas disease: 100 years after its discovery. Mem Inst Oswaldo Cruz 104: 31-40.
6) Prata A (2001) Clinical and epidemiological aspects of Chagas disease. Lancet Infect Dis 1:92-100.
7) Docampo R, Moreno SN (1984) Free radical metabolites in the mode of action of chemotherapeutic agents and phagocytic cells on *Trypanosoma cruzi*. Rev Infect Dis 6:223-38.
8) Teixeira AR, Arganaraz ER, Freitas Jr LH, Lacava ZG, Santana JM, et al. (1994) Possible integration of *Trypanosoma cruzi* kDNA minicircles into the host cell genome by infection.Mutat Res Fundam Mol Mech Mutagen 305:197-209.
9) Ramirez LE, Brener Z (1987) Evaluation of the rabbit as a model for Chagas' disease: I. Parasitological studies. Mem Inst Oswaldo Cruz 82:531-536.
10) Teixeira AR, Córdoba JC, Maior S, Solorzano E (1990) Chagas' disease: Lymphoma growth in rabbits treated with Benznidazole. Am J Trop Med 43:146-158.

11) Silva AM, Ramirez LE, Vargas M, Chapadeiro E, Brener Z (1996) Evaluation of the rabbit as a model for Chagas disease-II: Histopathologic studies of the heart, digestive tract and skeletal muscle. Mem Inst Oswaldo Cruz 91:199-206.

12) Almeida AB, Araujo PF, Bernal FM, de Cassia Rosa A, Valente SA, et al. (2019) Sexual transmission of American trypanosomes from males and females to naive mates. J Vis Exp 143:57985.

13) Araujo PF, Almeida AB, Pimentel CF, Silva AR, Sousa A, et al. (2017) Sexual transmission of American trypanosomiasis in humans: A new potential pandemic route for Chagas parasites. Mem Inst Oswaldo Cruz 112:437-446.

14) Guimaro MC, Alves RM, Rose E, Sousa AO, de Cassia Rosa A, et al. (2014) Inhibition of autoimmune Chagas-like heart disease by bone marrow transplantation. Plos Negl Trop Dis 8:e3384.

15) Teixeira AR, Gomes CC, Sa AA, Nascimento RJ, Lauria-Pires L, et al. *Trypanosoma cruzi* kDNA minicircle sequences integration into the vertebrate host genome: A biomarker for monitoring the efficacy of multidrug treatment of Chagas disease.

16) Sturm NR, Degrave W, Morel C, Simpson L (1989) Sensitive detection and schizodeme classification of *Trypanosoma cruzi* cells by amlification of kinetolast minicircle DNA sequences. Use in diagnosis of Chagas' disease. Mol Biochem Parasitol 33:205-214.

17) Moser DR, Kirchhoff LB, Donelson JE (1992) PCR amplification f mini- exon genes diferenciates *Trypanosoma cruzi* from *Trypanosoma rangeli*. J Clin Microbiol. 27:1447-1482.

18) Murthy VK, Dibbern KM, Campbell DA (1992) PCR amplification of mini-exon genes differentiates *Trypanosoma cruzi* from *Trypanosoma rangeli*. Mol Cell Probes 6:237-243.

19) Prado CM, Celes MR, Malvestio LM, Campos EC, Silva JS, et al. (2012) Early dystrophin disruption in the pathogenesis of experimental chronic Chagas cardiomyopathy. Microbes Infect 14:59-68.

20) Lewis MD, Kelly JM (2016) Putting infection dynamics at the heart of Chagas disease. Trends Parasitol 32:899-911.

21) Hecht MM, Nitz N, Araujo PF, Sousa AO, Rosa AD, et al. (2010) Inheritance of DNA transferred from American trypanosomes to human hosts. PLoS One. 5: e9181.

22) Árquez MA, Martin-Alonso S, Gorelick RJ, Scott WA, Acosta-Hoyos AJ, et al. (2020) Nucleocapsid protein precursors NCp9 and NCp15 suppress ATP-mediated rescue of AZT-terminated primers by HIV-1 reverse transcriptase. J Antimicrob Agents 64:10-128.

23) Tuli HS, Muobarak MJ, Thakral F, Sak K, Kumar M, et al. (2019) Molecular mechanisms of action of genistein in cancer. Front Pharmacol 10:1336.

24) Hiller BM, Marmion DJ, Gross RM, Thompson CA, Chavez CA, et al. (2021) Mitomycin-C treatment during differentiation of induced pluripotent stem cell-derived dopamine neurons reduces proliferation without compromising survival or function *in vivo*. Stem Cells Transl Med 10:278-290.

25) Bedi D, Henderson HJ, Manne U, Samuel T (2019) Camptothecin induces PD-L1 and immunomodulatory cytokines in colon cancer cells. Medicines 6:51.

26) Wang L, Gundelach JH, Bram RJ (2017) Cycloheximide promotes paraptosis induced by inhibition of cyclophilins in glioblastoma multiforme. Cell Death Dis 8:2807.

27) Ferreira de Oliveira JM, Pacheco AR, Coutinho L, Oliveira H, Pinho S, et al. (2018) Combination of etoposide and fisetin results in anti-cancer efficiency against osteosarcoma cell models. Arch Toxicol 92: 1205-1214.

28) Chakrabarty S, Nag D, Ganguli A, Das A, Ghosh Dastidar D, et al. (2019) Theaflavin and epigallocatechin-3-gallate synergistically induce apoptosis through inhibition of PI3K/Akt signaling upon depolymerizing microtubules in HeLa cells. J Cell Biochem 120:5987-6003.

29) Condezo GN, San Martín C. Bromodeoxyuridine labelling to determine viral DNA localization in fluorescence and electron microscopy: The case of adenovirus. Viruses 13:1863.

30) Forkosh E, Kenig A, Ilan Y (2020) Introducing variability in targeting the microtubules: Review of current mechanisms and future directions in colchicine therapy. Pharmacol Res Perspect 8:e00616.

31) Tarazi H, Saleh E, El-Awady R (2016) In-silico screening for DNA- dependent protein kinase (DNA-PK) inhibitors: Combined homology modeling, docking, molecular dynamic study followed by biological investigation. Biomed Pharmacother 83:693-703.

32) Ramos DF, Matthiensen A, Colvara W, Votto AP, Trindade GS, et al. (2015) Antimycobacterial and cytotoxicity activity of microcystins. J Venom Anim Toxins Incl Trop Dis 21:1-7.

33) Gonçalves AP, Videira A, Máximo V, Soares P (2011) Synergistic growth inhibition of cancer cells harboring the RET/PTC1 oncogene by staurosporine and rotenone involves enhanced cell death. J Biosci 36:639-648.

34) Simões-Barbosa A, Argañaraz ER, Barros AM, Rosa AD, Alves NP, et al. (2006) Hitchhiking Trypanosoma cruzi minicircle DNA affects gene expression in human host cells via LINE-1 retrotransposon. Mem Inst Oswaldo Cruz 101:833-843.

35) Cunha EL, da Silva Torchelsen FK, Cunha LM, de Oliveira MT, et al. (2019) Benznidazole, itraconazole and their combination in the treatment of acute experimental chagas disease in dogs. Exp Parasitol 204:107711.

36) de Jesus SM, Pinto L, Moreira FD, Nardotto GH, Cristofoletti R, et al. (2021) Pharmacokinetics of benznidazole in experimental chronic Chagas disease using the Swiss Mouse–Berenice-78 Trypanosoma cruzi strain model. Antimicrob Agents Chemother 65:10-128.

37) Molina I, Perin L, Sao Aviles A, de Abreu Vieira PM, da Silva Fonseca K, et al. (2020) The effect of benznidazole dose among the efficacy outcome in the murine animal model. A quantitative integration of the literature. Acta Tropica 201:105218.